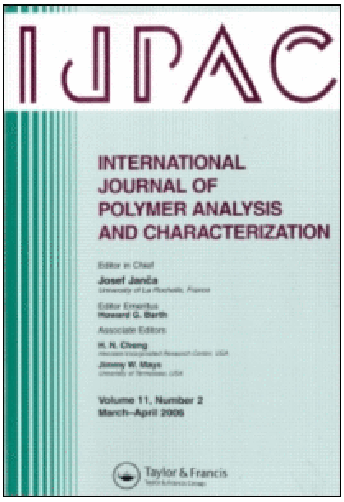

International Journal of Polymer Analysis and Characterization
Publication details, including instructions for authors and subscription information:
http://www.informaworld.com/smpp/title~content=t713646643

Development and Characterization of Polyamide-10, 6/Organoclay Nanocomposites

Adam Al-Mulla[a]
[a] Chemical Engineering Department, Kuwait University, Safat, Kuwait

To cite this Article Al-Mulla, Adam(2009) 'Development and Characterization of Polyamide-10, 6/Organoclay Nanocomposites', International Journal of Polymer Analysis and Characterization, 14: 6, 540 — 550
To link to this Article: DOI: 10.1080/10236660903086136
URL: http://dx.doi.org/10.1080/10236660903086136

International Journal of Polymer Anal. Charact., 14: 540–550, 2009
Copyright © Taylor & Francis Group, LLC
ISSN 1023-666X print
DOI: 10.1080/10236660903086136

Development and Characterization of Polyamide-10, 6/Organoclay Nanocomposites

Adam Al-Mulla
Chemical Engineering Department, Kuwait University, Safat, Kuwait

Abstract: Polyamide (PA-10, 6) with long alkane segments between amide groups was synthesized using sebacic acid and paradiaminobenzene. Organoclay was incorporated into the polyamide through the extrusion process. The structural characterizations, thermal properties, and molar mass of the polyamide nanocomposites were determined using X-ray diffraction, thermogravimetry (TG), and Fourier transform-infrared (FT-IR) spectroscopy, respectively. Tensile strength and Young's modulus of these polymers were measured using a Universal Test Instrument. FT-IR confirmed the presence of organics in the modified clay product. Wide-angle X-ray diffraction results indicated that the nanoclay platelets were agglomerated in the polyamide matrix. Mechanical behavior and degradation kinetics of the polyamide nanocomposites are reported and discussed.

Keywords: Mechanical properties; Polymer nanocomposites; Thermal degradation

INTRODUCTION

Aliphatic polyamide, or nylon, is an important member of the polymer family.[1] Almost all nylons exhibit relatively high modulus, strength,

Submitted 12 April 2009; accepted 3 June 2009.

This work was financially supported through project EC06/05 by the Research Administration at Kuwait University.

Correspondence: Adam Al-Mulla, Chemical Engineering Department, Kuwait University, P.O. Box 5969, Safat 13060, Kuwait. E-mail: adamalmulla@kuc01. kuniv.edu.kw

and toughness, as well as good temperature and abrasion resistance. The unique crystal structure, originating from the hydrogen bonds formed by –NH- and –CO-groups between adjacent molecular chains, results in nylon's high melting temperature, compared with other semicrystalline polymers such as polyethylene. Nylons tend to perform like polyethylene as the density of amide groups (–NHCO–) along the polymeric chains becomes very low.[1] The structure-property relationship of nylons can be varied based on the diacid and diamine chosen for the synthesis.[2–13]

Compounding polymers with inorganic materials has long been an interesting topic of scientific research and industrial application because inorganic materials can be used to improve the mechanical and barrier properties, high-temperature durability, and flammability resistance of the resultant polymer composites. Among various inorganic fillers, fibers, and anisotropic particles with large aspect ratios (length/diameter ratios), layered silicates have proven to be particularly effective in polymer matrix reinforcement.[3–5]

Layered silicates, such as montmorillonite, which is a structural group of 2:1 phyllosilicates, can be used for the synthesis of polymer-clay nanocomposites. The layer thickness of montmorillonites is around 1 nm, and the lateral dimensions range from 30 nm to several microns. The hydrophilic nature of clay surface makes it compatible with polymer matrices. The dispersion of clay is enhanced by ion exchange of cations, in the clay's intergalleries, with cationic surfactants, such as alkylammonium or alkylphosphonium. The cation exchange capacity for organoclay ranges between 0.80 and 1.50 mmol/g.

Nanocomposites can be processed by several methods such as solution polymerization, in situ polymerization, and melt compounding. Although nanocomposites of polymers having nonpolar chemical structure can be synthesized by solution and in situ polymerization, melt compounding is more advantageous in terms of its applicability to industrial processing techniques and elimination of the use of organic solvents from the processing medium. However, the type of extruder, residence time, shear intensity, chemical compatibility, and composite constituents are factors that influence effective use of the latter method. The presence of polar groups, in both the chemical structure of the polymer and the organic modifier, is of utmost importance for uniform dispersion of the organoclay. Some functional groups can be incorporated by using impact modifiers that function as compatibilizers, thus increasing the binding forces between the clay surface and the polymer and accordingly the toughness of nanocomposites.[4–8]

Generally, toughness is the only parameter of polymeric nanocomposites that is not enhanced by the presence of organoclay; it may even decrease. Moreover, it seems that possible fracture toughness enhancements are system specific, and thus no systematic predictive methodologies have been developed. Chen et al.[5] characterized toughness of maleated polypropylene-clay nanocomposites using the integral fracture mechanics approach. They observed a reduction in ductility and toughness as a result of constrained mobility of polymer chains in the vicinity of the clay surface. Nathani et al.[6] showed that combining polybutene with 5 wt.% clay primarily altered the micro mechanism of stress relaxation.

Although research has recently been devoted to the effect of organoclay addition on the crystallization behavior of the polyamide matrix,[3–6] the effect of organoclay on the morphology and the degradation behavior of PA-10, 6 has not been identified. These issues are addressed in this article using wide-angle X-ray diffraction (WAXD), thermogravimetric, and mechanical characterization. The correlation between the concentration of clay and the thermal properties of the nanocomposites is interpreted.

EXPERIMENTAL SECTION

Materials

Sebacic acid (Aldrich, USA) and paradiaminobenzene (Aldrich, USA) were used as received. Montmorillonite organoclay (Cloisite 30B) was purchased from Southern Clay Products (Texas, USA). Cloisite 30B, which was pretreated with dimethyl dehydrogenated tallow quaternary ammonium chloride, has a cation exchange capacity of 125 mmol/g.

Polymer Syntheses

Polyamide (PA-10, 6) was synthesized by melt polycondensation. First, sebacic acid was dissolved in absolute alcohol at 50°C and slowly added to a vigorously stirred solution of paradiaminobenzene in absolute alcohol. Subsequently, the paradiaminobenzene-sebazoate salt was formed. The mixture was stirred for a further 30 min before cooling to room temperature. The salt was filtered, repeatedly washed with absolute alcohol, and then dried in a vacuum desiccator. The treated salt was placed in a custom-made glass tube and a slight excess of paradiaminobenzene (about 1 mol %) was added to compensate for any possible losses. After fitting the glass tube into an autoclave, it was evacuated and flushed with nitrogen at 10 atm. The temperature was rapidly increased to 170°C (T_1) to initiate polymerization. After 2 h under these conditions, the autoclave was heated to 180°C (T_2). It was maintained at T_2 for another 2 h before the pressure was decreased to 5 atm. The autoclave was evacuated and the temperature was raised to 190°C (T_3), at which it was again maintained for 2 h. Finally, the autoclave was cooled and the resulting polymer removed.

Melt Compounding

PA-10, 6 was dried at 100°C under vacuum for 24 h prior to processing. The organoclay was dried for 12 h under vacuum at 60°C. PA-10, 6 nanocomposites (with 1, 3, and 5 wt.% organoclay) were prepared using a Collin Teach-Line (CSG 171T) single-screw extruder. Compounding was carried out at a screw speed of 100 rpm with a feed rate of 25 g/min. The temperature profile of the barrel was set to 220-235-250-230-225°C from hopper to die. The extrudate strands were cooled in a water bath and subsequently palletized. The product was kept in an oven at 60°C for 10 h prior to analysis.

CHARACTERIZATION

X-Ray Diffraction

WAXD was performed using a Rigaku D/MAX 2200/PC X-ray diffractometer at 40 kV and 40 mA, with a Cu Kα radiation source ($\lambda = 0.15418$ nm). WAXD patterns were recorded with step size of 0.01° from $2\theta = 1°$ to 10° at a scan rate of 1°/min. X-ray and Fourier transform-infrared (FT-IR) analysis of organoclay were carried out after thermal treatment at 250°C in an oven. The results were compared with X-ray and FT-IR analysis performed at room temperature. No addition or change in the peaks was noted in either.

Infrared Spectroscopy

FT-IR measurement was carried out on a Perkin-Elmer 1000 PC Fourier transform-infrared spectrometer.

Viscometry

The inherent viscosity of the synthesized polyamide was determined in dichloroacetic acid using an Ubbelohde viscometer (UBBEL10KC) at 25° ± 0.1°C, in accordance with testing standard ISO 3104.

Thermogravimetry

Thermogravimetric analysis (TGA) was performed on a TA-SDT 2960 Thermobalance using heating rates of 5, 10, 20, and 40°C/min, under nitrogen and air atmospheres (steady flow of 20 mL/min).

Mechanical Testing

Upon extrusion, the synthesized polymers were processed using an Allrounder 22 K injection molding machine (supplied by Arburg, Germany), at a temperature range of 230°–260°C and injection pressure of 800 bar, to produce tensile test specimens.

Tensile testing was performed at room temperature using a Tinius-Olsen Universal Test Instrument in accordance with testing standard ISO 527. The crosshead speed was set at 50 mm/min, except for Young's modulus determination, which was carried out at a crosshead speed of 1 mm/min.

RESULTS AND DISCUSSION

X-Ray Diffraction

The crystallinities calculated for PA-10, 6 were 42%, 14%, and 8%. WAXD patterns of (PA-10, 6)/3 wt.% organoclay nanocomposite showed crystallinities of 38%, 49%, and 58%, while (PA-10, 6)/5 wt.% organoclay nanocomposite exhibited crystallinities of 38%, 49%, and 59%. The WAXD results verified that crystallinity increased on incorporation of organoclay into the polyamide.

FT-IR

Infrared spectra of the polymers, shown in Figure 1, indicate that PA-10, 6 displays the following characteristic amide absorption bands: NH at 3400 and 1430, CONH at 1700 cm^{-1}. FT-IR confirms the presence of organics in the modified clay product (3650 and 3750 cm^{-1}) and provides the additional advantage of confirming the integrity of these organics. The infrared spectrum of organoclay displays bands around 3650 and 3750 cm^{-1} corresponding to OH groups. These bands are diminished when it is dispersed in the PA-10, 6 matrix.

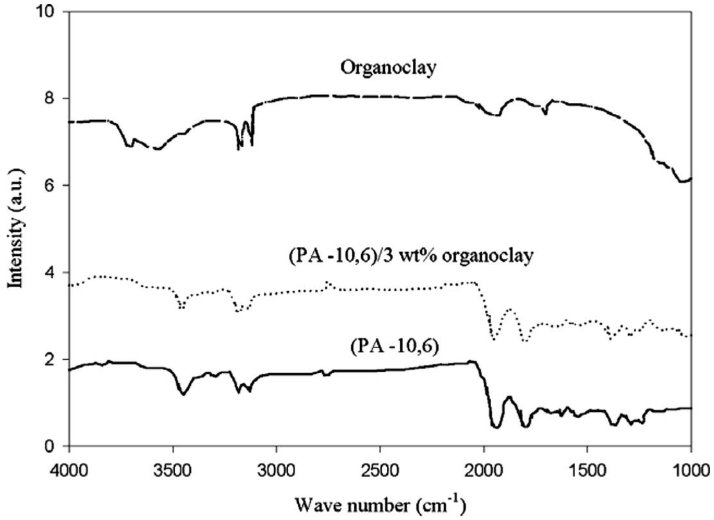

Figure 1. FT-IR spectra of organoclay, PA-10, 6, and (PA-10, 6)/3 wt.% organoclay.

Inherent Viscosity

The inherent viscosity of PA-10, 6, determined using an Ubbelohde viscometer, was found to be approximately 0.83 dL/g.

Thermogravimetric Analysis

The TG curve of the organoclay showed major weight loss over a range of 180°–510°C (Figure 2). The organic constituents in clay start to decompose within that range due to dehydroxylation of clay clusters and degradation of organic intercalant. This is supported by FT-IR spectra. Thus, both TGA and FT-IR provide direct evidence of organic uptake in the clay.

Single-stage decomposition characterizes the degradation of (PA-10, 6)/3 wt.% organoclay nanocomposite and PA-10, 6 under nitrogen and air (Figures 3 and 4). The degradation trends in nitrogen and air atmospheres were similar, as shown in Table I. The weight loss and maximum decomposition temperatures (T_{max}) under air and nitrogen atmospheres are higher for the nanocomposites than for the neat polymer. This indicates the greater thermal stability of the nanocomposites. These findings are consistent with the morphological observations that agglomerations in nanocomposites exhibited better thermal

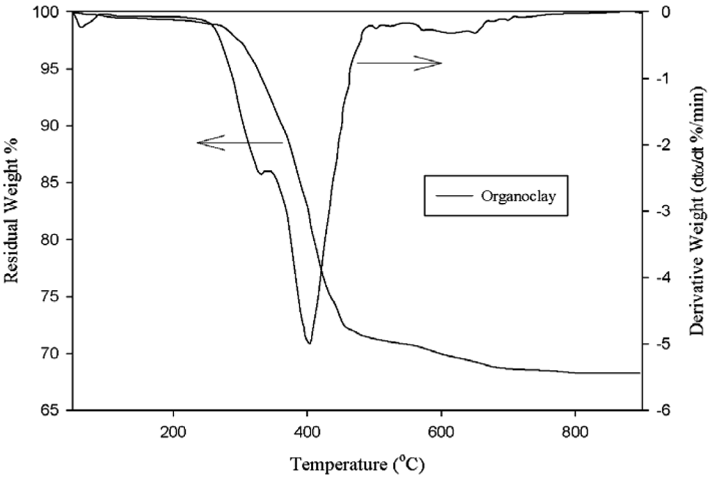

Figure 2. TG and DTG curves of organoclay under nitrogen atmosphere.

properties than the neat polyamides.[12] It has also been reported that the thermal properties of PA-10, 6 are close to those of nylon 6,6.[11] The onset temperature for degradation remained almost unchanged for the nanocomposite with 5 wt.% organoclay loading, despite changing the heating rate.

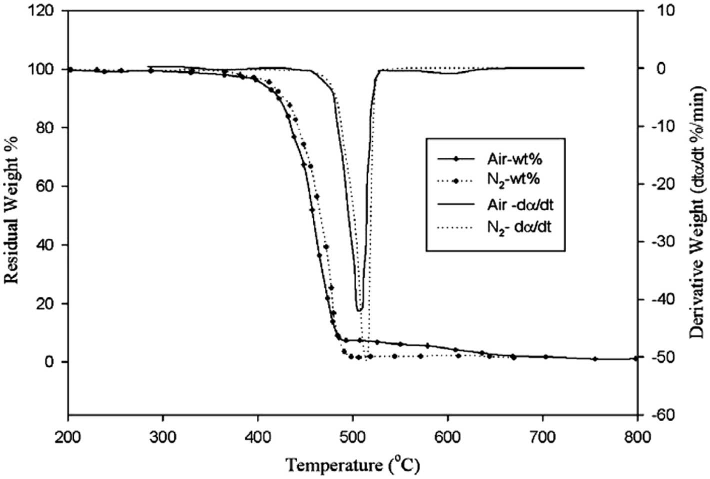

Figure 3. TG and DTG curves of (PA-10, 6)/3 wt.% organoclay under nitrogen and air at heating rate of 40°C/min.

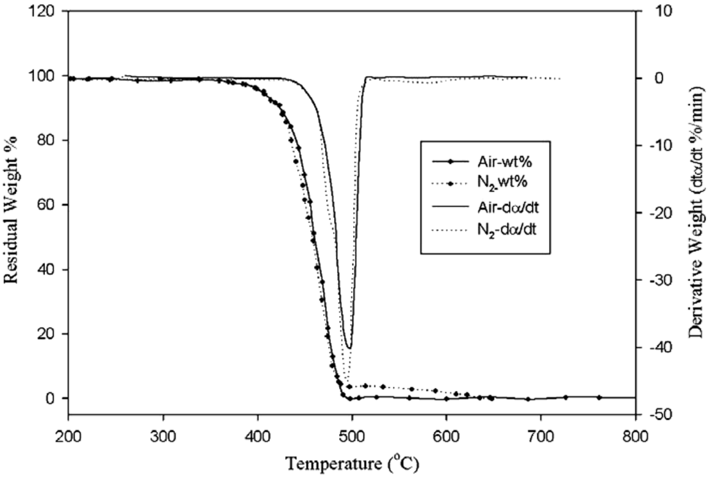

Figure 4. TG and DTG curves of PA-10, 6 under nitrogen and air at heating rate of 40°C/min.

The activation energy (E_a) for degradation was determined using the Kissinger method[13]:

$$\ln \frac{\beta}{T_{\max}^2} = \frac{E_a}{R}\left(\frac{1}{T_{\max}}\right) + \ln \frac{nAR(1-\alpha_m)^{n-1}}{E_a}$$

In the above equation, A is the collision factor, R is the molar gas constant, β is the heating rate, and n is the order of the degradation reaction (in this study, $n = 1$). In this method, the activation energy is obtained using $T_{\max}$, the temperature at which maximum degradation occurs, and α_m, the weight loss at $T_{\max}$, taken from derivative of TG (DTG) curves at several heating rates. The activation energy was

Table I. Thermal degradation characteristics for PA-10, 6 and its nanocomposites at 20°C/min

	Air			Nitrogen		
Clay content wt.%	$T_{5wt\%}$ (°C)	$T_{10wt\%}$ (°C)	$T_{\max}$ (°C)	$T_{5wt\%}$ (°C)	$T_{10wt\%}$ (°C)	$T_{\max}$ (°C)
0	396	418	460	400	418	468
1	400	420	462	410	425	473
3	402	422	466	407	423	470
5	404	424	467	408	424	472

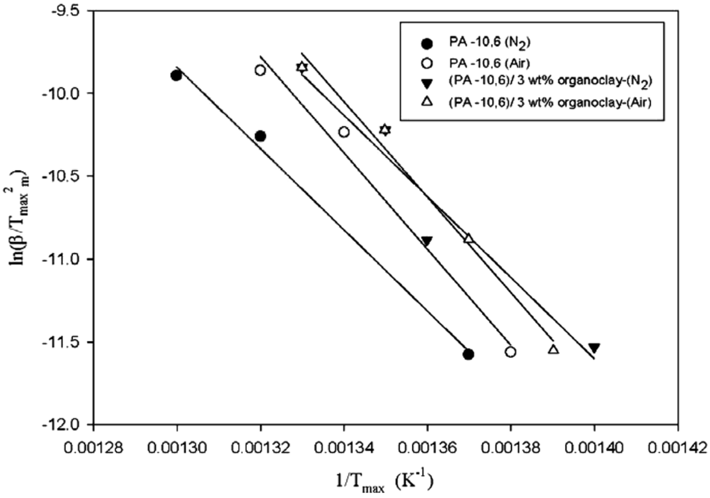

Figure 5. Determination of activation energy by Kissinger method for PA-10, 6 and (PA-10, 6)/3 wt.% organoclay under air and nitrogen.

determined from linear plots of $\ln(\beta/T_{max}^2)$ versus $1/T_m$ (Figure 5). The E_a values for PA-10, 6, (PA-10, 6)/1 wt.% organoclay, (PA-10, 6)/3 wt.% organoclay, and (PA 10, 6)/5 wt.% organoclay systems were found to be 170, 178, 182, and 186 kJ/mol under nitrogen and 178, 190, 210, and 218 kJ/mol under air, respectively.

MECHANICAL BEHAVIOR

Young's modulus (E) and tensile strength (σ_M) were obtained from the stress-strain curves of the samples tested. The presence of organoclay strongly affected the tensile properties of the polyamide. Neat PA-10, 6 exhibited cold-drawing beyond the yield stress and its strain-at-break was approximately 120%. The organoclay significantly influenced the failure mode. A loading of 1 wt.% of nanoclay reduced the ultimate strain at break to 23%. The nanocomposites containing 3 and 5 wt.% of organoclay failed immediately after reaching the yield stress at a strain-at-break value of approximately 8%. Figure 6 presents the tensile strength and Young's modulus as a function of clay content. Stiffness increased with increasing organoclay content. This can be ascribed to the competing effect between clay reinforcement and crystallinity.

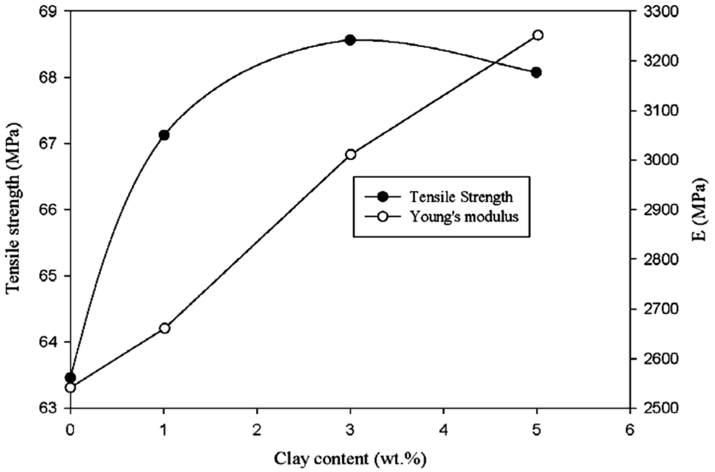

Figure 6. Tensile strength and Young's modulus of the nanocomposites as a function of organoclay content.

CONCLUSIONS

The polyamide PA-10, 6 was synthesized and then melt compounded to form nanocomposites with 1, 3, and 5 wt.% of organoclay. FT-IR confirms the presence and integrity of organics in the modified clay product. TGA revealed that the temperature at which maximum degradation occurs ($T_{\max}$) was higher in nitrogen than in air for all polymers. In general, $T_{\max}$ was higher for (PA-10, 6)/3 wt.% organoclay nanocomposite. The activation energies for degradation were slightly higher for (PA-10, 6)/5 wt.% organoclay nanocomposite than for other systems, under both air and nitrogen atmospheres. This indicates that agglomerated clay particles do not significantly enhance the thermal stability of the polyamide matrix. Mechanical analysis showed that the presence of organoclay influenced the failure mode. Incorporation of organoclay into PA-10, 6 generally reduced its toughness. The nanocomposites were stiffer than the neat polymer as a result of the enhancement of crystallization. The decrease in tensile strength was proportional to organoclay loading.

REFERENCES

[1] Jouffret, F., and P.-J. Madec. (1996). Polyamide synthesis by ester aminolysis. I. A new route for nylon-6,6 synthesis. *J. Polym. Sci. Part A Polym. Chem.* **34**, 2363–2370.

[2] Cho, J. W., and D. R. Paul. (2001). Nylon 6 nanocomposites by melt compounding. *Polymer* **42**, 1083–1094.

[3] Sinha Ray, S., and M. Okamoto. (2003). Polymer/layered silicate nanocomposites: A review from preparation to processing. *Prog. Polym. Sci.* **28**, 1539–1641.

[4] Fornes, T. D., P. J. Yoon, D. L. Hunter, H. Keskkulaand, and D. R. Paul. (2002). Effect of organoclay structure on nylon 6 nanocomposite morphology and properties. *Polymer* **43**, 5915–5933.

[5] Chen, L., S.-C. Wong, and S. Pisharath. (2003). Fracture properties of nanoclay-filled polypropylene. *J. Appl. Polym. Sci.* **88**, 3298–3305.

[6] Nathani, H., A. Dasariand, and R. D. K. Misra. (2004). On the reduced susceptibility to stress whitening behavior of melt intercalated polybutene-clay nanocomposites during tensile straining. *Acta Mater.* **52**, 3217–3227.

[7] Dasari, A., Z.-Z. Yu, M. Yang, Q.-X. Zhang, X.-L. Xie, and Y.-W. Mai. (2006). Micro- and nano-scale deformation behavior of nylon 66-based binary and ternary nanocomposites. *Compos. Sci. Technol.* **66**, 3097–3114.

[8] Hassan, A., N. Othman, M. U. Wahit, L. J. Wei, A. R. Rahmat, and Z. A. M. Ishak. (2006). Maleic anhydride polyethylene octene elastomer toughened polyamide 6/polypropylene nanocomposites: Mechanical and morphological properties. *Macromol. Symp.* **239**, 182–191.

[9] Lincoln, D. M., R. A. Vaiaand, and R. Krishnamoorti. (2004). Isothermal crystallization of nylon-6/montmorillonite nanocomposites. *Macromolecules* **37**, 4554–4561.

[10] Wu, T.-M., and C.-S. Liao. (2000). Polymorphism in nylon 6/clay nanocomposites. *Macromol. Chem. Phys.* **201**, 2820–2825.

[11] Levchik, S. V., E. D. Weil, and M. Lewin. (1999). Thermal decomposition of aliphatic nylons. *Polym. Int.* **48** (7), 532–557.

[12] Njuguna, J., K. Pielchowski, and S. Desai. (2008). Nanofiller-reinforced polymer nanocomposites. *Polym. Adv. Technol.* **19** (8), 947–959.

[13] Kissinger, H. E. (1957). Reaction kinetics in differential thermal analysis. *Anal. Chem.* **29**, 1702–1706.